

# Transport of exotic anti-nuclei: I- Fast formulae for $\bar{p}$ fluxes

D. Maurin,<sup>1</sup> R. Taillet,<sup>2</sup> and C. Combet<sup>3</sup>

<sup>1</sup>*Dipartimento di Fisica Teorica, Università di Torino,*

*Istituto Nazionale di Fisica Nucleare, via P. Giuria 1, I-10125 Torino, Italy\**

<sup>2</sup>*Laboratoire de Physique Théorique LAPTH, Annecy-le-Vieux, 74941, France*

*Université de Savoie, Chambéry, 73011, France<sup>†</sup>*

<sup>3</sup>*Dublin Institute for Advanced Studies DIAS, 5 Merrion Square, Dublin 2, Ireland*

*Laboratoire d'Astrophysique, Observatoire de Grenoble LAOG, BP 53 F-38041 Grenoble Cedex 9, France<sup>‡</sup>*

(Dated: January 25, 2020)

The secondary Galactic cosmic ray anti-proton flux calculated with different propagation models is fairly consistent with data, and the associated propagation uncertainty is small. This is not the case for any  $\bar{p}$  exotic component of the dark matter halo (also see the companion paper). Whereas detailed propagation models are mandatory if the ultimate goal is to explain an excess, simpler and faster approximate formulae for  $\bar{p}$  are an attractive alternative to full calculations, when it comes, for example, to putting conservative constraints on new physics in this channel.

PACS numbers: 98.38.Cp, 98.35.Pr, 96.40.-z, 98.70.Sa, 96.50S-, 96.50sb, 95.30.Cq, 12.60.Jv, 95.35.+d

## I. MOTIVATION

The first positive detection of  $\bar{p}$  at the end of the seventies [1, 2, 3] boosted the interest for indirect searches of new physics in the low energy  $\bar{p}$  spectrum. After 25 years of efforts and improvements both in measurements and theoretical calculations, the data at low energy (up to a few GeV) are now well accounted for [4]. However, at higher energy, calculations tend to predict less  $\bar{p}$  than observed [5] but more data are desirable to confirm this deviation.

The uncertainty of the  $\bar{p}$  standard secondary flux mainly comes from nuclear physics [6], whereas that of astrophysical origin is already small—less than a few percents—and is expected to decrease even more as new B/C measurements are available. In contrast, the  $\bar{p}$  exotic flux—from exotic sources following the dark matter distribution—is plagued by the degeneracy in the propagation parameters, the corresponding uncertainty being as large as two orders of magnitude [7] at low energy.

Galactic cosmic ray  $\bar{p}$  flux is only a part of a larger picture. In the absence of a smoking-gun signature (such as that proposed, e.g., in [8]), all the searches (direct or indirect signatures) must be combined to find evidence for a precise dark matter candidate. Furthermore, if direct detection is ever achieved, the dark matter character of a newly discovered particle can be probed through all possible indirect signatures. However, until propagation is better understood and constrained, it may not be worth using refined—and sometimes time consuming—models whose result will anyway be crippled by these large uncertainties. This is especially true when one has to scan

as efficiently as possible the huge parameter space existing, for example, in SUSY theories.

The goal of this paper is to provide approximate formulae for the propagated  $\bar{p}$  exotic fluxes : these formulae are reasonably accurate, fast to compute and easy to implement. They have to be thought as an easy-to-use tool, for phenomenologists interested in beyond-the-standard-model theories and wishing to quickly check that any new physics model on the market does not violate the  $\bar{p}$  constraint<sup>1</sup> (as was done for example in [9] for many signals). We use the framework of the diffusion/convection model with constant wind, which we already used in [4, 7, 10, 11]. The paper is organized as follows:

- In Sec. II, we briefly remind the salient ingredients of the constant wind/diffusion model as used and detailed in Barrau et al. [11], for exotic  $\bar{p}$ . A first approximation consists in switching off all energy redistribution processes (§II B).
- In Sec. III, energy redistributions are discarded and two alternative formulations are proposed. One is the propagator approach (§ III A), which is an exact description, and the second is the 1D-model (§ III B), which assumes a constant dark matter distribution in the Galaxy. Performances and limitations of these two models are then given (§III C).
- In Sec. IV the above results are implemented in a numerical routine provided with the paper. This routine calculates the exotic flux for a given set of propagation parameters, and compares it to a “reference measured” background  $\bar{p}$  flux.

---

\*Electronic address: maurin@to.infn.it

<sup>†</sup>Electronic address: taillet@lapp.in2p3.fr

<sup>‡</sup>Electronic address: ccombet@obs.ujf-grenoble.fr

---

<sup>1</sup> A companion paper further elaborates on uncertainties, reinforcing the pertinence to use, at this stage and for this task, approximate models rather than full calculations.

## II. 2D-MODEL WITH CONSTANT WIND $V_c$

Cosmic ray fluxes are determined by the transport equation, as given, e.g., in Berezhinskii et al. [12]. For stable species, the gas detailed distribution in the disk is not of primary importance, and we use the so-called thin-disk approximation. Cylindrical symmetry is assumed, and we use a general source term  $\mathcal{S}_{\text{prim}}(r, z)$ .

The same diffusion coefficient holds throughout the Galaxy,

$$K(E) = \beta K_0 \mathcal{R}^\delta \quad (\mathcal{R} = pc/|Z|e \text{ is the rigidity}).$$

A galactic wind  $V_c$  of constant magnitude, directed outwards along  $z$ , is also included. Denoting the differential density  $dN/dE$  as  $N$  and omitting energy losses leads to

$$\left\{ -K \Delta + V_c \frac{\partial}{\partial z} + \Gamma_{\text{tot}} \delta(z) \right\} N = \mathcal{S}_{\text{prim}}(r, z, E). \quad (1)$$

The quantity  $\Gamma_{\text{tot}} = \sum_{\text{ISM}} n_{\text{ISM}} v \cdot \sigma_{\text{ISM}}^{\bar{p}}$  is the destruction rate of  $\bar{p}$  in the thin gaseous disk ( $n_{\text{ISM}} = \text{H, He}$ ). The boundary conditions are  $N(z = L, r) = 0$  and  $N(r = R, z) = 0$ . The parameters of the model are i) the halo size  $L$  of the Galaxy, ii) the normalization of the diffusion coefficient  $K_0$ , iii) its slope  $\delta$ , iv) the constant galactic wind  $V_c$  and finally v) the level of reacceleration through the Alfvénic speed  $V_a$  (see, e.g., Maurin et al. [13]).

### A. Full solution including energy losses

#### 1. Solutions

For the sake of completeness, the semi-analytical solution is rewritten below. However, we choose a slightly different form than in Barrau et al. [11]<sup>2</sup>, this new expression being more suitable for the numerical implementation of energy losses. In cylindrical coordinates, expressed along the usual first order Bessel expansion (see details in [11],  $\zeta_i$  is the  $i$ -th zero of  $J_0$ )

$$N^{\text{prim}}(r, z) = \sum_{i=1}^{\infty} N_i^{\text{prim}}(z) J_0 \left( \zeta_i \frac{r}{R} \right),$$

where

$$N_i^{\text{prim}}(z) = \mathcal{N}_i(0) e^{\frac{V_c z}{2K}} \frac{\sinh \left[ \frac{S_i}{2} (L - z) \right]}{\sinh \left( \frac{S_i L}{2} \right)} + e^{-\frac{V_c}{2K} (L - z)} \frac{\sinh(S_i z / 2) y_i(L)}{\sinh(S_i L / 2) K S_i} - \frac{y_i(z)}{K S_i}. \quad (2)$$

<sup>2</sup> Note that there is a misprint in Eq. (A.5) of [11]. The product  $K A_i S_i$  should read  $K S_i$ .

Halo model	$\alpha$	$\beta$	$\gamma$	$r_c$ [kpc]
Cored isothermal	2	2	0	4
<i>à la</i> NFW [14, 15]	1	3	1	25
<i>à la</i> Moore [16, 17]	1	3	1.2	30

TABLE I: Parameters to be plugged into Eq. (5) to obtain various modelings of the dark matter distribution profile in the Milky Way.

Each  $\mathcal{N}_i(0)$  is solution of a differential equation

$$\mathcal{N}_i(0) = N_i(0) - \frac{2h}{K} \left[ b(E) \frac{d\mathcal{N}_i(0)}{dE} + c(E) \frac{d^2 \mathcal{N}_i(0)}{dE^2} \right],$$

which is solved by means of a numerical scheme detailed in Donato et al. [4]. The terms  $b(E)$  and  $c(E)$  are given in Maurin et al. [13]. The remaining quantities are defined as follows:

$$N_i(0) \equiv e^{-\frac{V_c L}{2K}} \frac{y_i(L)}{A_i \sinh(S_i L / 2)}; \quad (3)$$

$$y_i(z) \equiv 2 \int_0^z e^{\frac{V_c}{2K} (z - z')} \sinh \left[ \frac{S_i}{2} (z - z') \right] q_i(z') dz';$$

$$S_i \equiv \sqrt{\frac{V_c^2}{K^2} + 4 \frac{C_i^2}{R^2}}; \quad A_i \equiv 2h \Gamma_{\text{tot}} + V_c + K S_i \coth \left( \frac{S_i L}{2} \right).$$

Note that, in the above expression,  $q_i(z)$  are the Fourier-Bessel coefficients of  $\mathcal{S}_{\text{prim}}(r, z)$ . Some numerical issues about the convergence of the series, when using cuspy dark matter halo, are underlined in App. A.

#### 2. Dark matter profile

The exotic source term follows the generic form

$$\mathcal{S}_{\text{prim}}(r, z) = Q^{\bar{p}}(E) \times f_{\text{Source}}(r, z), \quad (4)$$

where the spatial dependence—in cylindrical coordinates  $(r, z)$ —of the source term is normalized to 1 at Solar position. For evaporation of Primordial Black Holes or for SUSY-like particles,  $f_{\text{Source}}(r, z)$  is equal to

$$f_{\text{Dark}}(r, z) \quad \text{or} \quad f_{\text{Dark}}^2(r, z),$$

where  $f_{\text{Dark}}(r, z)$  is the dark matter distribution profile, also normalized to 1 at Solar position. Notice that any information such as, e.g., the relic density, the fraction of the dark matter halo filled by the new candidate or any quantity related to the dark matter candidate is irrelevant at this stage: it is absorbed in the term  $Q(E)$ . The right factors should be implemented accordingly when using the approximate formulae.

The following generic form is taken for the profile:

$$f_{\text{Dark}}(r, z) = \left( \frac{R_\odot}{\sqrt{r^2 + z^2}} \right)^\gamma \left( \frac{r_c^\alpha + R_\odot^\alpha}{r_c^\alpha + \sqrt{r^2 + z^2}^\alpha} \right)^{(\beta - \gamma)/\alpha}, \quad (5)$$

Set	$\delta$	$K_0$ (kpc <sup>2</sup> Myr <sup>-1</sup> )	$L$ (kpc)	$V_c$ (km s <sup>-1</sup> )
<i>max</i>	0.46	0.0765	15	5
<i>best</i>	0.7	0.0112	4	12
<i>min</i>	0.85	0.0016	1	13.5

TABLE II: Propagation parameters consistent with B/C data [10]. The set labeled *best* corresponds to the best fit to B/C data, while those labeled *min* and *max* correspond to sets which give minimum and maximum exotic fluxes [7].

where parameters are given in Tab. I. The distance to the galactic center is set to  $R_\odot = 7.5$  kpc, a value that several methods seem to converge to [18]. This is at variance with the usually recommended  $R_\odot = 8.0$  kpc (e.g. [19]), but has no impact on the derived results below. Indeed,  $R_\odot$  is just another parameter, and our approximate formulae will perform well for any user-preferred value  $\approx 8.0$  kpc.

### 3. Propagation parameters

Only a sub-region of the propagation parameter space is compatible with B/C data (e.g., Maurin et al. [10]). Using the above 2D-model, it was found for example that  $\delta$ , the slope of the diffusion coefficient, was constrained to lie in the range  $0.46 - 0.85$  [10]. The accuracy of the approximate formulae given in this work is studied for this sub-region of parameter space only. In particular, Tab. II gathers the set of parameters leading to the maximum/minimum exotic fluxes (see companion paper), as well as the configuration corresponding to the best fit to B/C data.

### B. Neglecting energy redistributions

In this section, the realistic dark matter profile (as described in Sec. II A 2) is implemented in the full 2D-model, switching-on then off energy redistributions. The calculated flux corresponds to the set of equations given in Sec. II A. Notice that when energy redistributions are neglected, the quantity  $\mathcal{N}_i(0)$  to plug in Eq. (2) becomes merely the quantity  $N_i(0)$  defined in Eq. (3). We use the generic term *error* for the difference between solutions calculated with and without energy redistributions.

*a. Expected effect of energy redistributions* As energy redistributions act on the spectrum, it is not obvious to disentangle which of the following input parameters—source spectrum, profile, transport coefficients—is the most crucial regarding *error*. On a general footing, energy losses and tertiary contributions tend to replenish the low energy tail in case of a dropping flux at these same energies (that is why it has a very important effect on the secondary  $\bar{p}$  [4]). On the other hand, reacceleration tends to smear the spectrum at low and high energy in case of a flux peaking at GeV energy. Taking all these

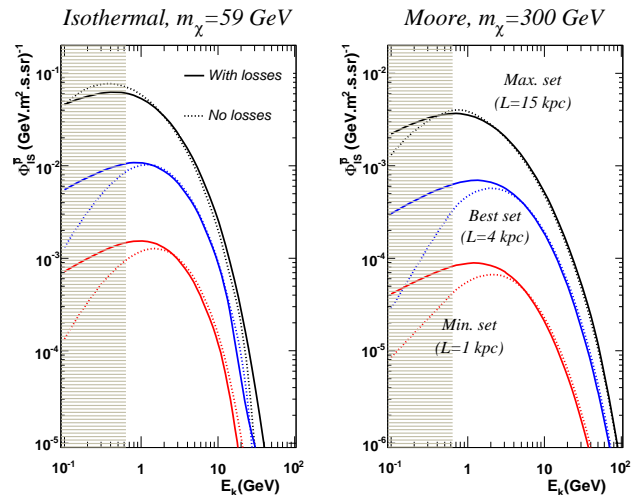


FIG. 1: For both panels: from top to bottom, the *max*, *best* and the *min* propagation sets (see Tab. II). The dashed lines correspond to the propagated fluxes without energy redistributions, while solid lines correspond to the same propagated exotic fluxes, but with energy redistributions (energy losses, reacceleration, tertiary source term) taken into account. The shaded regions correspond to  $\bar{p}$  which cannot reach Earth (because of solar modulation).

points into account, the following remarks—regarding energy redistributions—can be made:

**Source spectrum:** in most cases, PBH-like source spectra do not decrease at low energy (Fig. 3 of Barrau et al. [11]), whereas SUSY-like candidates are quite flat (see Fig. 6 of Donato et al. [7]). Hence, taking various source spectra is not expected to play a major role in *error*.

**Dark matter profile:** be it for SUSY-like or PBH-like source terms, changing the profile mostly changes the normalization of the propagated spectrum, not the overall shape. Hence, no significant contribution to *error* is expected.

**Propagation parameters:** as a general rule when fitting B/C, small  $L$  are associated with a large Galactic wind and a small reacceleration parameter, while this is the reverse for large  $L$ . Large winds—which are more efficient as the energy diminishes—decrease low energy fluxes, making them more sensitive to energy redistribution effects. This has a dominant effect on *error* compared to the two others.

*b. Behavior of error* Figure 1 displays the two resulting fluxes for various input configurations. The decrease of the flux observed at low energy for the best and minimal propagation set is due to the Galactic wind. For the smallest  $L$ , the propagated flux is steeper (because of larger wind values, see Tab. II), hence more affected by

energy redistributions. Notice that only for  $L = 15$  kpc, where  $V_c = 5 \text{ km s}^{-1}$ , can the shape of the source spectrum be truly appreciated. As expected, the *error* calculated when varying the neutralino mass or the dark matter profile is less important.

The *error* can be as large as a factor of  $\sim 5$  at very low energy, but we remind that these are  $\bar{p}$  at IS energies, which cannot reach Earth because of solar modulation (shaded region in Fig. 1). Above a few hundreds of MeV (lowest IS energy reachable for low solar activity), the difference obtained is always  $\lesssim 50\%$ . Above a few tens of GeV, energy redistributions are always negligible, so that *error* tends to zero. In between, the only situation when *error* can be large corresponds to a steep spectrum dropping rapidly to zero, which is uninteresting in the perspective of detecting any excess.

*c. Conclusion* A model neglecting energy redistributions provides an accurate enough description to determine exotic fluxes. This result is in agreement with the intuitive idea that exotic species, in order to reach us, cross the gaseous disk less often than standard ones, implying that they are less subject to energy redistributions.

### III. OTHER ALTERNATIVES AND SIMPLIFICATIONS

Only neglecting energy redistributions leads to a marginal gain for the calculation. Still many Bessel orders are required as before and issues about convergence remain unchanged, while ending up with an approximate result. Any serious alternative formulation needs to do better than that.

#### A. Propagator (no side boundaries: $R \rightarrow \infty$ )

In [20], the expression for the propagator corresponding to the same 2D diffusion equation (without energy redistributions) was extracted in the limit<sup>3</sup>  $R \rightarrow \infty$ . We remind that the propagator  $\mathcal{G}(r, z)$  is solution of

$$\left\{ -K\Delta + V_c \frac{\partial}{\partial z} + n\delta(z)v\sigma \right\} \mathcal{G} = \delta(\vec{r} - \vec{r}').$$

Once the propagator is known, the flux at  $z = 0$  (the flux only depends on the relative distance to the source) can

<sup>3</sup> The propagator for finite  $R$  was presented and used in [21] to obtain the most likely *origin* of exotic  $\bar{p}$  detected on Earth. This propagator relied on Bessel expansion. For practical use,  $R \gg 1$  was required, so that it was equivalent to the form presented below. However, in the context of a quick and simple formulae, it is largely outperformed (in term of convergence properties) by the one presented in this paper.

be calculated for any source term through the integration

$$N(0) = 2 \int_0^{2\pi} \int_0^L \int_0^R \mathcal{G}(r', \theta', z') q(r', \theta', z') r' d\theta dr' dz'.$$

The density due to a point source located in  $(r, z)$  measured by an observer located at  $z_{\text{obs}} = 0$  (and  $r_{\text{obs}} = 0$ ), after diffusion through a halo limited by two parallel planes at  $z = \pm L$ , is given by

$$\mathcal{G}(r, z) = \frac{\exp^{-k_v z}}{2\pi K L} \times \sum_{n=0}^{\infty} c_n^{-1} K_0(r\sqrt{k_n^2 + k_v^2}) \sin k_n L \sin k_n(L - z) \quad (6)$$

where  $K_0$  is the modified Bessel function of the second kind,  $k_n$  is solution of

$$2k_n \cos k_n L = -k_d \sin k_n L, \quad (7)$$

$c_n$  is defined as

$$c_n = 1 - \frac{\sin k_n L \cos k_n L}{k_n L} \quad (8)$$

and

$$k_v \equiv V_c / (2K).$$

The quantity  $k_d$  depends on the total destruction rate  $\Gamma_{\text{tot}}$  and the constant convective wind  $V_c$ :

$$k_d \equiv 2h \Gamma_{\text{tot}} / K + 2k_v. \quad (9)$$

This propagator was never used in our previous studies as we wished to take properly into account energy redistributions. However, we have shown that the latter only feebly affect the exotic fluxes : it then becomes an interesting alternative to the more complicated and more prone to numerical instability formalism given in Sec. II A.

#### B. The 1D model

We now consider an infinite disk whose density and source distribution do not depend on  $r$ . The constant wind diffusion transport equation for a generic source term  $\mathcal{Q}(z, E) = q(z)Q(E)$  without energy redistributions reads

$$-K \frac{d^2 N}{dz^2} N + V_c \frac{dN}{dz} + 2h\delta(z)\Gamma_{\text{tot}} N = q(z)Q(E). \quad (10)$$

As we do not take into account energy losses, the energy  $E$  is decoupled from the spatial dependence  $z$  so that it is omitted. In 1D-models, only  $z$ -dependence is allowed. For simplicity, it is further assumed that the source term  $q$  is constant throughout the Galaxy. We

refer the reader to the companion paper for details of the calculation. The final solution is

$$\begin{cases} N(z) = \frac{qL}{V_c} \left\{ \frac{(1 + \alpha + \xi) \cdot (1 - e^{-\alpha(1 - \frac{z}{L})})}{\alpha + \xi(1 - e^{-\alpha})} + \frac{z}{L} - 1 \right\} \\ N(0) = \frac{qL}{V_c} \left\{ \frac{1 - (1 + \alpha)e^{-\alpha}}{\alpha + \xi(1 - e^{-\alpha})} \right\} \end{cases} \quad (11)$$

where  $\xi = h\Gamma_{\text{tot}}L/K$  and  $\alpha = V_cL/K$ .

### C. Comparison with full 2D formulae

We focus on fluxes measured at the solar neighbourhood only, i.e. at  $z_{\text{obs}} = 0$  and  $r_{\text{obs}} = R_{\odot}$  (or merely  $z_{\text{obs}} = 0$  for the 1D-model). Energy redistributions are switched-off in the 2D-model for comparison.

#### 1. Propagator

By construction, it provides an exact description of the transport (when energy redistributions are discarded). This was checked explicitly, comparing the propagator result with the 2D-semi-analytical model for a realistic DM profile. Both calculations are almost always in perfect agreement. A less perfect match is obtained in the case where the halo size has the same extension of the radial extension of the Galaxy  $R$ . In that case, we no longer have  $L \ll R$  and the side boundary starts affecting the flux, as discussed in [21, 22].

#### 2. 1D-model

The flux is evaluated at  $z = 0$ . Figure 2 compares the 1D-model to the result from the 2D semi-analytical model:

- For PBH-like sources, as long as  $L \lesssim 7$  kpc, the 1D-model provides a very good estimate of exotic  $\bar{p}$  fluxes.
- For SUSY-like sources, 1D-models are sufficient for very small halo size  $L$  only.

These very good matches are easily understood if we remember that the closest boundary defines a cut-off distance: anti-nuclei from sources located further away are exponentially suppressed [21, 22]. Hence, we are only sensitive to the average value of  $f_{\text{Dark}}$  within this cut-off distance, close to one at solar position, as taken in the 1D-model. Obviously, as soon as contributions close to the Galactic center are less suppressed, this equivalence breaks down; all the more for SUSY-like source terms compared to PBH-like source terms (because of the square in  $f_{\text{Dark}}$ ).

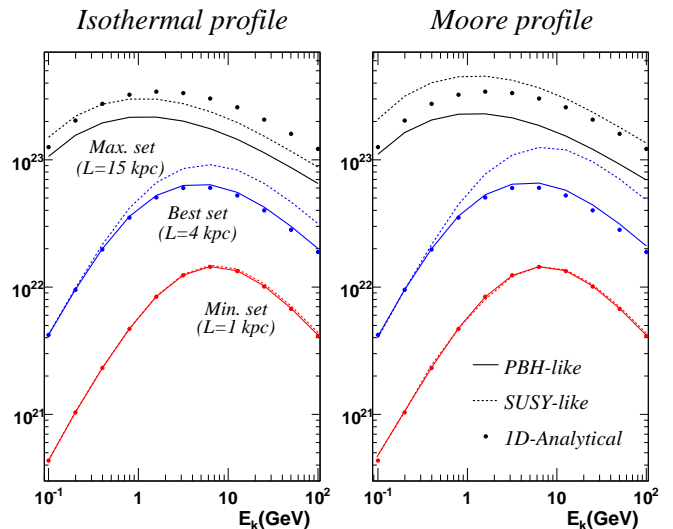


FIG. 2: Both figures correspond to the ratio of the  $\bar{p}$  exotic flux to its source term (in arbitrary units) as a function of the kinetic energy. Lines: 2D-semi-analytical model, no energy redistributions (Sec. II A) for PBH-like (solid lines) or SUSY-like (dashed lines) sources. Symbols: Eq. (11), 1D-model (independent on the dark matter profile). The three sets of propagation parameters are those of Tab. II. Left panel: Isothermal profile; right panel: Moore profile.

## IV. C++ ROUTINES

Taking advantage of these two formalisms, a routine in C++ is given, to evaluate the  $\bar{p}$  flux from any input dark matter profile, source spectrum, and propagation parameters. They can be retrieved from the arXiv website, along with the present paper. The main routine returns the ratio of the propagated IS exotic flux (for a user-specified source term) to the standard  $\bar{p}$  IS flux, i.e.

$$\Omega \equiv \Phi_{\text{exotic}}^{\bar{p} \text{ -IS}} / \Phi_{\text{standard}}^{\bar{p} \text{ -IS}}.$$

The input parameters are the following:

- Propagation parameters:  $K_0$  ( $\text{kpc}^2 \text{ Myr}^{-1}$ ),  $\delta$ ,  $V_c$  ( $\text{km s}^{-1}$ ) and  $L$  (kpc);
- Exotic source spectrum:  $Q_{\text{exotic}}^{\bar{p}}(E_k)$  ( $\text{GeV}^{-1} \text{ m}^{-3} \text{ s}^{-1}$ ) and the corresponding kinetic energy  $E_k$  (GeV);
- Dark matter profile: the parameters  $\alpha$ ,  $\beta$  and  $\gamma$  (see I) as well as the source type (SUSY-like or PBH-like).

The resulting fluxes, in  $(\text{GeV m}^2 \text{ s sr})^{-1}$ , are obtained at solar position  $(R_{\odot}, 0)$ . We chose to express all fluxes as IS quantities to free the user from using a modulation routine. The IS background  $\bar{p}$  spectrum is described using a fit function (see App. C) and matches the data using a force-field scheme [4]. There are uncertainties associated with the choice of the modulation/demodulation scheme,

but they are not likely to be much larger than the errors associated with nuclear physics or with the approximations discussed in this paper.

We remind that the range of propagation parameters given in Tab. II implies that large uncertainties remain on exotic fluxes (without mentioning the fact that the constant wind model is probably not the *definitive* model for the Galaxy). To make conservative estimates, we recommend the reader to use the *min* set of propagation parameters associated with the condition  $\Omega \gtrsim 1$  to exclude his exotic model. Regarding the most likely  $\bar{p}$  exotic flux in this model, it is given by the *best* set ( $L = 4$  kpc, see Tab. II). In any case, it has to be kept in mind that energy smaller than  $\sim 600$  MeV IS correspond to  $\bar{p}$  which are almost never detected on Earth.

## V. CONCLUSION

Given the present accuracy of propagation parameters, exotic anti-proton fluxes suffer large uncertainties (see also the companion paper). This limits the benefit of a detailed calculation, which can be expensive in term of computational power, when repeated thousands of times.

We showed that energy redistributions could be safely discarded providing results accurate at the level of  $\lesssim 50\%$ , for all relevant parts of the exotic  $\bar{p}$  spectrum, as long as IS energies are not taken smaller than  $\lesssim 1$  GeV (leading to  $\lesssim 100$  MeV energies once modulated).

Doing so opens the possibility to use *analytical* formulae:

- either the approximate 1D-model, which gives the correct flux as long as  $L \lesssim 7$  kpc for PBH-like sources, or  $L \lesssim 1$  kpc for SUSY-like sources;
- or the propagator, which is an exact description (the expense of the 3D numerical integration is not crippling and can be handled quickly).

The advantage of the 1D-model is its compactness and simplicity (no dependence on the dark matter profile), while the second approach is more accurate. The former could be preferred in situations where speed is a decisive factor, e.g. when scanning a large parameter space as in SUSY studies. Moreover, in order to be conservative in exclusion studies, small halo size should be taken. In particular conservative estimates are made when using the 3<sup>rd</sup> line of Tab. II: this is exactly the regime where 1D-formulae hold. Such formulae could be easily implemented in “indirect detection” codes such as, e.g., micrOMEGAs (Belanger et al. [23]).

So far, these formulae are valid only in the framework of the constant wind model. Although all the discussions were developed with respect to  $\bar{p}$  fluxes, all results can be transposed almost without any modification to the  $\bar{d}$  case (the total cross section has to be taken accordingly to the species considered). A piece of code was supplied for the  $\bar{p}$  case (implementation for the  $\bar{d}$  should be provided in

a forthcoming publication, after a careful reevaluation of the standard flux).

## Acknowledgments

We thank E. Nezri for useful discussions held during the GDR-SUSY meeting, and J. Lavalle for a careful reading of the manuscript.

## APPENDIX A: NUMERICAL INSTABILITIES IN THE 2D MODEL

Dealing with Bessel function is a source of numerical instabilities in many cases. They happen if i)  $R \gg L$  or ii) too many Bessel orders are used, or even, in the case of spiky dark matter halo, if too few orders are used. As the propagator formulation below allows cross-checks, we take the opportunity to give a few recommendations regarding the parameters to use:

1. always keep  $R$  in the range  $5L \lesssim R \lesssim 10L$ . The limit  $10L$  is set to avoid numerical instabilities while the limit  $5L$  allows to avoid boundary effects [21] (the boundary in  $R$  decreases the flux at most to a few tens of percent for a Moore profile).
2. For a smooth profile (e.g. Isothermal), 20 Bessel functions give an almost perfect convergence.
3. For NFW and Moore profiles in the case of SUSY-like candidate (50 Bessel functions are sufficient for PBH-like candidate), following a procedure inspired by [24], we replace in the calculation the standard profile, by

$$g_{\text{Dark}}^2(r) = \begin{cases} r_{\text{th}}^{2\gamma} \cdot f_{\text{Dark}}^2(r_{\text{th}}) \cdot \pi^2 \Upsilon \cdot \frac{\sin(\pi r/r_{\text{th}})}{\pi r/r_{\text{th}}} & \text{if } r \leq r_{\text{th}} \\ f_{\text{Dark}}^2(r) & \text{otherwise;} \end{cases} \quad (\text{A1})$$

with  $\Upsilon = (3 - 2\gamma)^{-1}$  and  $\gamma$  is the slope from Tab. I. In these expressions,  $r \equiv \sqrt{r_{\text{cyl}}^2 + z^2}$  denotes the spherical coordinate. In any case, we find that, setting  $r_{\text{th}} = 400$  pc, 50 Bessel functions give a good accuracy, while 100 functions allow to reach a very good match.

## APPENDIX B: CHECK OF PROPAGATOR FORMULAE

The validity of the propagator is checked in a simple case, by integrating it over a constant source term  $q(r, z) = 1$  in order to compare with the 1D formula.

### 1. Purely diffusive regime: $V_c = 0$

a. *No spallations,  $k_d = 0$*

In that case,  $k_n \equiv (n+1/2)\pi$ . Integration over  $z$  (using  $q(r, z) = 1$ ) leads to

$$\int_{-L}^L dz \mathcal{G}(r, z) = \frac{1}{\pi KL} \sum_{n=0}^{\infty} \frac{(-1)^n}{k_n} K_0(k_n r), \quad (\text{B1})$$

and integration over the disk  $\int_0^R 2\pi r dr$  gives

$$N(0) = \frac{2}{KL} \sum_{n=0}^{\infty} \frac{(-1)^n}{k_n^3} \int_0^{k_n R} y K_0(y) dy.$$

Using the properties  $\int y K_0(y) dy = -yK_1(y)$  and  $yK_1(y) \sim 1$  when  $y \rightarrow 0$ ,

$$N(0) = \frac{2}{KL} \sum_{n=0}^{\infty} \frac{(-1)^n}{k_n^3} [1 - k_n R K_1(k_n R)].$$

Finally, for  $R \gg 1$ , the expression becomes

$$N(0) = \frac{2}{KL} \sum_{n=0}^{\infty} \frac{(-1)^n}{k_n^3} = \frac{2L^2}{\pi^3 K} \sum_{n=0}^{\infty} \frac{(-1)^n}{(n+1/2)^3}.$$

The infinite sum has the value  $\sum (-1)^n / (n+1/2)^3 = \pi^3/4 \approx 7.7515$ , so that

$$N(0) = \frac{L^2}{2K} \equiv N^{\text{1D-model}}(0).$$

Note that, in the infinite sum, the first term  $n = 0$  is equal to 8, so that it only slightly overshoots the exact value. Hence, only a few terms are required in the sum to converge quickly to the correct value.

b. *With spallations,  $k_d = 2h\Gamma_{\text{tot}}/K$*

There is no longer a simple expression for  $k_n$ . Following a similar derivation as the one above, we find

$$N(0) = \frac{4}{Kk_d L} \sum_{n=0}^{\infty} \left( 1 - \frac{\sin k_n L \cos k_n L}{k_n L} \right)^{-1} \times \frac{\cos k_n L}{k_n^2} [\cos k_n L - 1]. \quad (\text{B2})$$

A numerical check of this sum confirms that Eq. (B2) equals the 1D-model, i.e. Eq. (11) where  $V_c = 0$ . This means that

$$\sum_{n=0}^{\infty} \frac{\cos(k_n L) [\cos(k_n L) - 1]}{k_n L (k_n L - \sin(k_n L) \cos(k_n L))} = \frac{k_d L}{4(2 + k_d L)}.$$

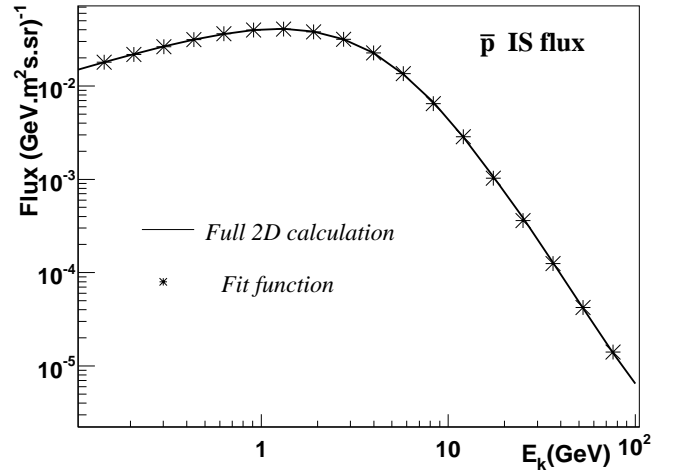


FIG. 3: Interstellar standard  $\bar{p}$  flux along with its fit function as given by Eq. (C1).

### 2. Diffusive/convective regime: $V_c \neq 0$

The integration leads to quite similar results as for the previous case (with spallations). A numerical check confirms that Eq. (11) is recovered.

Note that the integration should be performed for sources located at all  $r$ , with  $r \rightarrow \infty$ . In practice, it is sufficient (and it saves a lot of computational time) to integrate only from 0 to  $10L$  (or from 0 to  $\min(10L, 10L_{\text{eff}})$  in the case of a convective wind, where  $L_{\text{eff}} \equiv K/V_c$ ). In that case, a grid of  $\sim 25$  points for all coordinates ( $r$ ,  $z$  and  $\theta$ ) is sufficient to reach the correct result.

### APPENDIX C: COMPACT FIT TO $\bar{p}$ SECONDARY FLUX

Whatever the propagation parameters, as soon as the right B/C ratio is obtained, the same  $\bar{p}$  secondary flux will always be obtained (Donato et al. [4]). Still, some uncertainties exist (mostly due to cross-section uncertainties), but they are at the level of a few tens of percent [4]. Moreover, the  $\bar{p}$  secondary flux obtained by many teams are also in fair agreement.

If we have in mind to scan and exclude, for example, points in the SUSY parameter space, a fitted function to describe the standard  $\bar{p}$  flux is good enough. Indeed, there really is no need in calculating again and again the same final quantity with various input parameters (the propagation parameters). The following fit function can be considered to be the correct  $\bar{p}$  secondary flux, regardless of the propagation model chosen. Setting  $x \equiv \log(E_k)$  where  $E_k$  is the kinetic energy in GeV, the standard IS  $\bar{p}$  flux in  $(\text{GeV m}^2 \text{ s sr})^{-1}$  is parameterized

as

$$\Phi_{\text{standard}}^{\bar{p} - \text{IS}} = \begin{cases} \exp\left(\sum_{i=0}^4 C_i x^i\right) & \text{if } E_k < 11 \text{ GeV}, \\ \exp(D_0 x^{D_1}) & \text{otherwise;} \end{cases} \quad (\text{C1})$$

The constants are defined by  $C_0 = -3.211$ ,  $C_1 = 0.12145$ ,  $C_2 = -0.2728$ ,  $C_3 = -0.075265$ ,  $C_4 = -0.007162$ , and  $D_0 = -2.02735$  and  $D_1 = 1.16463$ . The fit is shown in Fig. 3.

- [1] R. L. Golden, S. Horan, B. G. Mauger, G. D. Badhwar, J. L. Lacy, S. A. Stephens, R. R. Daniel, and J. E. Zipse, *Physical Review Letters* **43**, 1196 (1979).
- [2] A. Buffington, S. M. Schindler, and C. R. Pennypacker, *Astrophys. J.* **248**, 1179 (1981).
- [3] E. A. Bogomolov, N. D. Lubianaia, V. A. Romanov, S. V. Stepanov, and M. S. Shulakova, in *International Cosmic Ray Conference* (1982), pp. 146–149.
- [4] F. Donato, D. Maurin, P. Salati, A. Barrau, G. Boudoul, and R. Taillet, *Astrophys. J.* **563**, 172 (2001).
- [5] M. Boezio, V. Bonvicini, P. Schiavon, A. Vacchi, N. Zampa, D. Bergström, P. Carlson, T. Francke, S. Grinstein, M. Suffert, et al., *Astrophys. J.* **561**, 787 (2001).
- [6] R. Duperray, B. Baret, D. Maurin, G. Boudoul, A. Barrau, L. Derome, K. Protasov, and M. Buénerd, *Phys. Rev. D* **71**, 083013 (2005).
- [7] F. Donato, N. Fornengo, D. Maurin, P. Salati, and R. Taillet, *Phys. Rev. D* **69**, 063501 (2004).
- [8] G. Bertone, A. R. Zentner, and J. Silk, *Phys. Rev. D* **72**, 103517 (2005).
- [9] Y. Mambrini and E. Nezri, hep-ph/0507263 (2005).
- [10] D. Maurin, F. Donato, R. Taillet, and P. Salati, *Astrophys. J.* **555**, 585 (2001).
- [11] A. Barrau, G. Boudoul, F. Donato, D. Maurin, P. Salati, and R. Taillet, *Astronomy and Astrophys.* **388**, 676 (2002).
- [12] V. S. Berezinskii, S. V. Bulanov, V. A. Dogiel, and V. S. Ptuskin, *Astrophysics of cosmic rays* (Amsterdam: North-Holland, 1990, edited by Ginzburg, V.L., 1990).
- [13] D. Maurin, R. Taillet, and F. Donato, *Astronomy and Astrophys.* **394**, 1039 (2002).
- [14] J. F. Navarro, C. S. Frenk, and S. D. M. White, *Astrophys. J.* **490**, 493 (1997), astro-ph/9611107.
- [15] J. F. Navarro, E. Hayashi, C. Power, A. R. Jenkins, C. S. Frenk, S. D. M. White, V. Springel, J. Stadel, and T. R. Quinn, *MNRAS* **349**, 1039 (2004), astro-ph/0311231.
- [16] B. Moore, T. Quinn, F. Governato, J. Stadel, and G. Lake, *MNRAS* **310**, 1147 (1999), astro-ph/9903164.
- [17] J. Diemand, M. Zemp, B. Moore, J. Stadel, and M. Carollo, *MNRAS* **364**, 665 (2005), astro-ph/0504215.
- [18] S. Nishiyama, T. Nagata, S. Sato, D. Kato, T. Nagayama, N. Kusakabe, N. Matsunaga, T. Naoi, K. Sugitani, and M. Tamura, *ArXiv Astrophysics e-prints* (2006), astro-ph/0607408.
- [19] W.-M. Yao, C. Amsler, D. Asner, R. Barnett, J. Beringer, P. Burchat, C. Carone, C. Caso, O. Dahl, G. D’Ambrosio, et al., *Journal of Physics G* **33**, 1+ (2006), URL <http://pdg.lbl.gov>.
- [20] R. Taillet, P. Salati, D. Maurin, and E. Pilon, *Difusion in a slab: different approaches* (2004), URL <http://www.citebase.org/abstract?id=oai:arXiv.org:physics/0>
- [21] D. Maurin and R. Taillet, *Astronomy and Astrophys.* **404**, 949 (2003), astro-ph/0212113.
- [22] R. Taillet and D. Maurin, *Astronomy and Astrophys.* **402**, 971 (2003), astro-ph/0212112.
- [23] G. Belanger, F. Boudjema, A. Pukhov, and A. Semenov (2006), hep-ph/0607059.
- [24] A. Barrau, P. Salati, G. Servant, F. Donato, J. Grain, D. Maurin, and R. Taillet, *Phys. Rev. D* **72**, 063507 (2005).